FIFTH INTERNATIONAL CONGRESS ON SOUND AND VIBRATION
DECEMBER 15-18, 1997
ADELAIDE, SOUTH AUSTRALIA

PREDICTION OF GROUND VIBRATION
INDUCED BY HIGH-SPEED TRAIN OPERATION

Hirokazu TAKEMIYA
Environmental and Civil Engineering, Okayama University, Okayama, Japan

Kazuya GODA
Toyo Construction Co., Ltd

ABSTRACT

In this paper the ground vibration induced by train running on track is dealt with as an environmental problem. The concerned 3-dimensional wave propagation in soils is solved by using the Fourier transform method in space and time. The solution satisfying the given boundary condition is obtained in the transformed domain by applying the FEM and BEM solution method. The back transformation with respect to frequency is made analytically while from the wave number domain into the space is carried out by the discrete wave number method with application of the FFT algorithm.

As an example, an embankment type train truck on layered soils is analyzed. The field measurements are conducted and used to calibrate the simulation results in the frequency domain since various vibration sources are involved.

1. INTRODUCTION

Connecting cities by high speed trains is pursued along with the increasing demand of mass transportation of people and cargoes. Speeding up of train operation on track may produce unexpected environmental problems such as vibrations to propagate toward the neighborhood, disturbing people and troubling sensitive machines along the track. The quantitative prediction of the vibration level and the countermeasure for reduction, if necessary, is of importance for the better environment.

The train induced vibration is characterized by moving loads of specific frequency contents and soil conditions.[1,2] In fact, various sources are involved: the wheel distance, number of cars, speed of operation, drift of rails, structural born vibration, etc.[3,4] The 3-dimensional analysis of vibration propagation is crucial in view of the effect of moving loads. However, mostly, the transversal section of the track and underlain soils may be assumed identical along track, which makes the so-called 2.5-dimenaionsal analysis possible.

An embankment type train track is focused in this study. Due to the complex boundary condition the finite element modeling is adopted for this portion. The underlying layered soils are treated by the boundary elements procedure with discretization along the depth for the

Green function involved. The harmonic analysis is executed for the specified frequencies. The solution procedure is to use the Fourier transform to expand the wave propagation in space into the wave numbers. The back transformation from the wave number domain into the space is carried out analytically along the track direction while by the discrete wave number method in the transverse direction to it. The FFT algorithm is applied from the frequency to the time domain transformation.

The field measurements are conducted on ground vibrations along the Shinkan-sen track and the nearby. These data are used to calibrate the computer simulation results for the better prediction.

2. FORMULATION

The following assumptions are made for the present analysis:
(1) An embankment type train track overlying a layered soil is considered.
(2) An identical transversal cross section extends all along the track direction.
(3) The soil medium behaves linearly with hysteretic internal damping effect.
(4) The moving train load of certain frequencies is represented by the traction distribution on the surface of embankment track.

Fig.1 illustrates the discretized modeling of the embankment type train track and the underlain layered soils. Fig.2 indicates the track loading area due to trains.
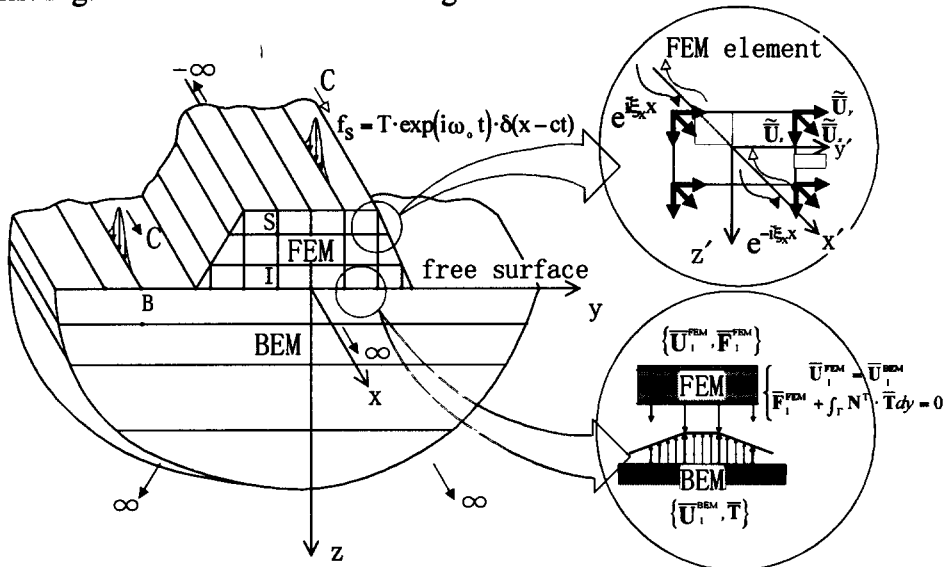

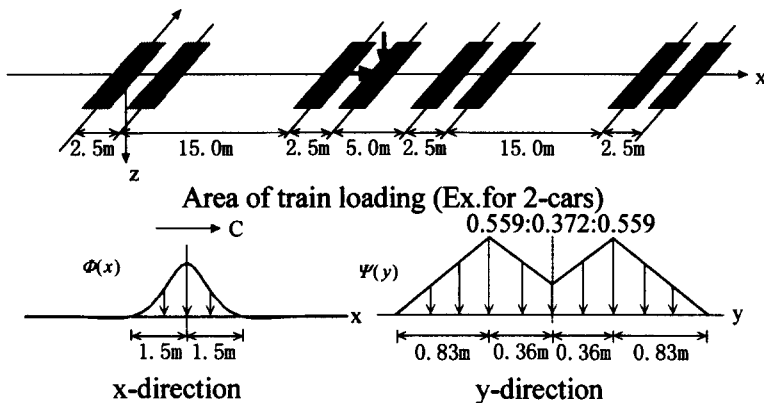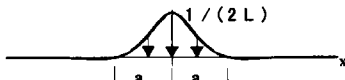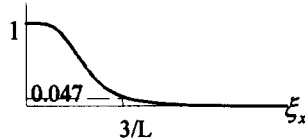Fig.1 FEM-BEM discretized modeling for dynamic analysis

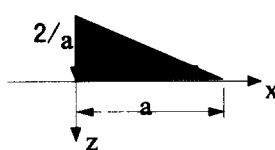Area of train loading (Ex.for 2-cars)
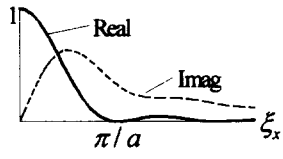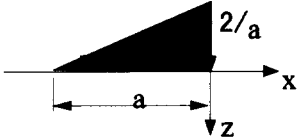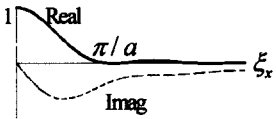

x-direction y-direction

Fig. 2 Train loads on track

Harmonic solution method is applied.[2] Assume that a moving load of frequency ω_0 with the distributions in x- and y-direction are given, respectively, by $\Phi(x - c\,t)$ and $\Psi(y)$.

$$f(x, y, z, t) = \Psi(y)\,\Phi(x - c\,t)\,\delta(z)\,exp(i\,\omega_0 t)\,T \qquad (1)$$

in which $\delta(z)$ expresses the Dirac's delta function and T represents the stress intensity. Table 1 describes the distributions functions considered.

Table. 1   Stress distribution[2]

Type	Space domain	Wave number domain	$S(\xi_{yk}, y)$ in Eq.(5) ; Upper for even and lower for odd of $\widetilde{\widetilde{u}}$
I	$\Phi(x) = \dfrac{1}{\sqrt{2}L}\exp(-\left|\dfrac{x}{L}\right|)\sin(\left|\dfrac{x}{L}\right| + \dfrac{\pi}{4})$ $a = \dfrac{3\pi L}{4}$, $L = \sqrt[4]{\dfrac{4EI}{K}}$ 	$\widetilde{\Phi}(\xi) = \dfrac{4}{4 + (\xi L)^4}$ 	
II	$\Phi(x) = \dfrac{2}{a}(1 - \left|\dfrac{x}{a}\right|) \quad 0 \le x \le a$ 	$\widetilde{\Phi}(\xi) = \dfrac{2}{(a\xi)^2}(1 - e^{i\xi a} + i\xi a)$ 	$\begin{Bmatrix} S(\xi_{yk}, y) \\ S(\xi_{yk}, y) \end{Bmatrix} = \dfrac{2}{(a\xi)^2}\begin{Bmatrix} 1 \\ -i \end{Bmatrix} \cdot$ $\left[(1 - \cos(a\xi_{yk}))\begin{Bmatrix}\cos(\xi_{yk} y) \\ \sin(\xi_{yk} y)\end{Bmatrix} \right.$ $\left. + (a\xi_{yk} - \sin(a\xi_{yk}))\begin{Bmatrix}\sin(\xi_{yk} y) \\ \cos(\xi_{yk} y)\end{Bmatrix} \right]$
III	$\Phi(x) = \dfrac{2}{a}(1 + \left|\dfrac{x}{a}\right|) \quad -a \le x \le 0$ 	$\widetilde{\Phi}(\xi) = \dfrac{2}{(a\xi)^2}(1 - e^{-i\xi a} - i\xi a)$ 	$\begin{Bmatrix} S(\xi_{yk}, y) \\ S(\xi_{yk}, y) \end{Bmatrix} = \dfrac{2}{(a\xi)^2} \cdot$ $\left[(1 - \cos(a\xi_{yk}))\begin{Bmatrix}\cos(\xi_{yk} y) \\ \sin(\xi_{yk} y)\end{Bmatrix} \right.$ $\left. - (a\xi_{yk} - \sin(a\xi_{yk}))\begin{Bmatrix}\sin(\xi_{yk} y) \\ \cos(\xi_{yk} y)\end{Bmatrix} \right]$

The Fourier transformed expression to Eq.(1) becomes

$$\widetilde{f}(\xi_x, \xi_y, z, \omega) = \dfrac{2\pi \widetilde{\Psi}(\xi_y)\widetilde{\Phi}(\xi_x)\delta(z)}{c}\,\delta\left(\xi_x - \dfrac{\omega - \omega_0}{c}\right) T \qquad (2)$$

with ξ_x and ξ_y denoting respectively the wave numbers in x- and y-direction. The response in the transformed domain can be solved , as

$$\widetilde{u}(\xi_x, \xi_y, z, \omega) = \widetilde{s}(\xi_x, \xi_y, z, \omega)\delta\left(\xi_x - \dfrac{\omega - \omega_0}{c}\right) \qquad (3)$$

This expression indicates that for a constant train speed a fixed wave number is associated with the wave propagation in the x-direction . The response in space and time domain is therefore obtained by the inverse transform of

$$u(x, y, z, t) = \dfrac{1}{8\pi^3}\int_{-\infty}^{+\infty}\int_{-\infty}^{+\infty}\widetilde{u}\left(\dfrac{\omega - \omega_0}{c}, \xi_y, z, \omega\right)\exp(i\dfrac{\omega_0 x}{c})\exp(-i\xi_y y)\exp\left\{i\omega\left(t - \dfrac{x}{c}\right)\right\}d\xi_y d\omega \quad (4)$$

The discretized solution method is taken for the track and underlain soils[5]: the embankment structure is modeled by the finite elements in the y-z plane that includes the x-directional wave number ξ_x while the underlain layered soils by the thin layered elements along the z-direction. For computing the Green function of the layered soil, the wave number integral in y-direction is replaced by the summation over the discrete wave numbers for the transformed domain solution $\widetilde{\overline{u}}$, i.e.,

$$\overline{U}(x,y,z,\omega) = \frac{1}{4\pi^2} \sum_{k=0}^{K} \widetilde{\overline{u}}\left(\frac{\omega-\omega_0}{c}, \xi_{yk}, z, \omega\right) S(\xi_{yk}y) \exp\left(-i\frac{\omega-\omega_0}{c}x\right) \Delta\xi_y \tag{5}$$

with
$$\xi_{yk} = \frac{2\pi k}{L} \quad (k = 0,1,2,\cdots,K)$$

in which $\Delta\xi_y = 2\pi/L$, L is the specific length, and $S(\xi_{yk}y)$ is determined for given loading types II and III in Table 1.

The governing equation in the hybrid procedure is expressed in the wave number and frequency domain as[5]

$$\begin{bmatrix} \mathbf{K}_{SS} & \mathbf{K}_{SI} & \mathbf{0} \\ \mathbf{K}_{IS} & \mathbf{K}_{II}^{FEM} + \mathbf{K}_{II}^{BEM} & \mathbf{K}_{IB} \\ \mathbf{0} & \mathbf{K}_{BI} & \mathbf{K}_{BB} \end{bmatrix} \begin{Bmatrix} \overline{\mathbf{U}}_S \\ \overline{\mathbf{U}}_I \\ \overline{\mathbf{U}}_B \end{Bmatrix} = \begin{Bmatrix} \overline{\mathbf{F}}_S^0 \\ \overline{\mathbf{F}}_I^0 \\ \overline{\mathbf{F}}_B^0 \end{Bmatrix} \tag{6}$$

in which the subffices S, I and B indicate respectively the finite element nodes, interface nodes and the boundary element nodes. The time domain solution is finally obtained from the solution of Eq.(6) by applying the Fast Fourier Transform.

4. COMPUTER SIMULATION

In order to investigate the interaction effect between the embankment track and the underlain soil, a preliminary simulation was first made by assuming a unit patch load as described in Eq.(1) on the track in Fig.3. The source frequency of f_0=10 Hz is assumed to move with the speed c=216 km/s (60m/s).

The case for flat tracks has been investigated elsewhere.[2] The embankment track, when compared, shows some evidence of the dynamic interaction of the embankment with the underlain soils depending on their impedance ratio. Fig.4 is the z-directional response time histories. The

Fig.3 An embankment type train track

origin of the time scale is set at which the moving load passes the focused place. In the case of Vs=100 m/s for the soil layer the response is larger than other cases. The case for Vs=400 m/s for the soil layer indicates an impulsive-like response at the embankment top due to the stiffness ratio between the embankment and the underlain soils, while a small smoothed response on the free field. The response for the Vs=200 m/s for the soil layer is between those for Vs=100 m/s and Vs=400 m/s for the soil layer.

Fig.5 is the corresponding Fourier amplitudes. The predominant frequencies for the soil layer of Vs=400 m/s are 9Hz and 12Hz, those for Vs=200 m/s are 8Hz and 15Hz. These
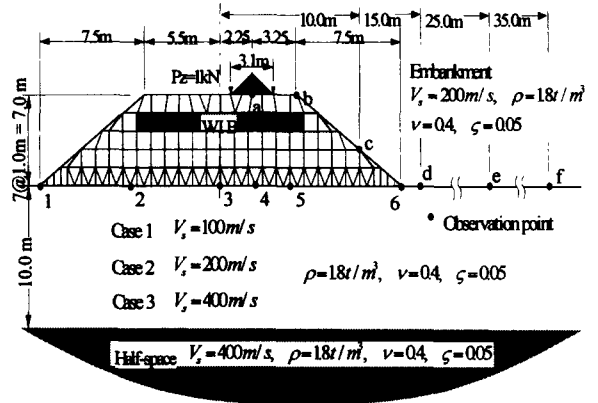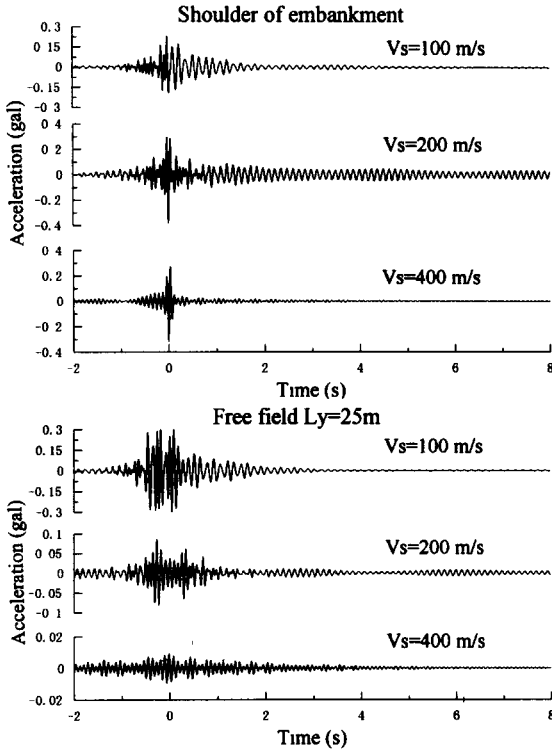
Fig. 4 Time histories of z-directional acceleration (c=60 m/s, f_0=10 Hz)
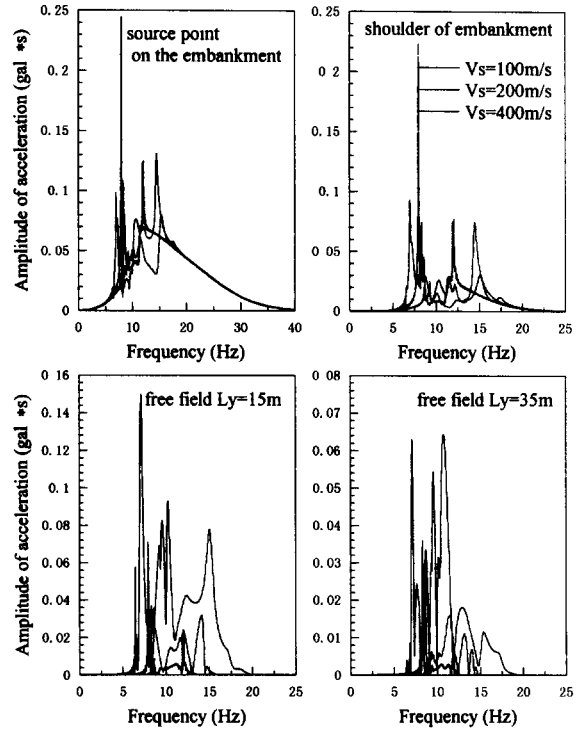

Fig; 5 Frequency contents of x-directional acceleration (c=60 m/s, f_0=10 Hz)

frequencies correspond to the values as obtained from the Doppler formula

$$f = \frac{V_r}{V_r \pm c} f_0 \tag{7}$$

in which f_0 is the exerting frequency and V_r is the Rayleigh wave velocity for the surface layer; namely, they are 8.6Hz and 11.9Hz for the soil layer of Vs=400 m/s, 7.6Hz and 14.8Hz for the Vs=200 m/s. The predominant frequencies for the case of Vs=100 m/s are noted as 7Hz, 10.5Hz and 16Hz, and the first and the third frequencies coincide with those obtained from the intersection of the dispersion curves for the in-plane and out-of-plane waves with the moving speed curve.[6] The frequency 10.5Hz may be due to the dynamic interaction between the embankment and the underlain soil layer. This case indicates the most characteristic of the two layered soils.

Referring to the maximum acceleration in Fig.6, in the case of Vs=100 m/s for soil layer the response at the foot of embankment is large compared to the small response of Vs=200, 400 m/s. The z-directional response is big and the y-directional is around the half and the x-directional is the smallest. The attenuation trend is different depending on the impedance ratio of the soil layer with the embankment. For the information of these dynamic interaction, the interface response is investigated. In the case of Vs=400 m/s only a peak response appears at the embankment center due to the constraint by the stiff underlain soil. In the case of Vs=100 m/s a large response is allowed all along the interface due to the flexible behavior of the underlain soils. In view of the nature of the Green function of a layered medium, the increasing response trend in the order of Vs= 400, 200 and 100 m/s is understood.

The authors have previously proposed a vibration reduction method by installing a wave impeding block (WIB) of concrete material inside embankment.[6] It is noted this works effectively for halving the large acceleration at embankment.
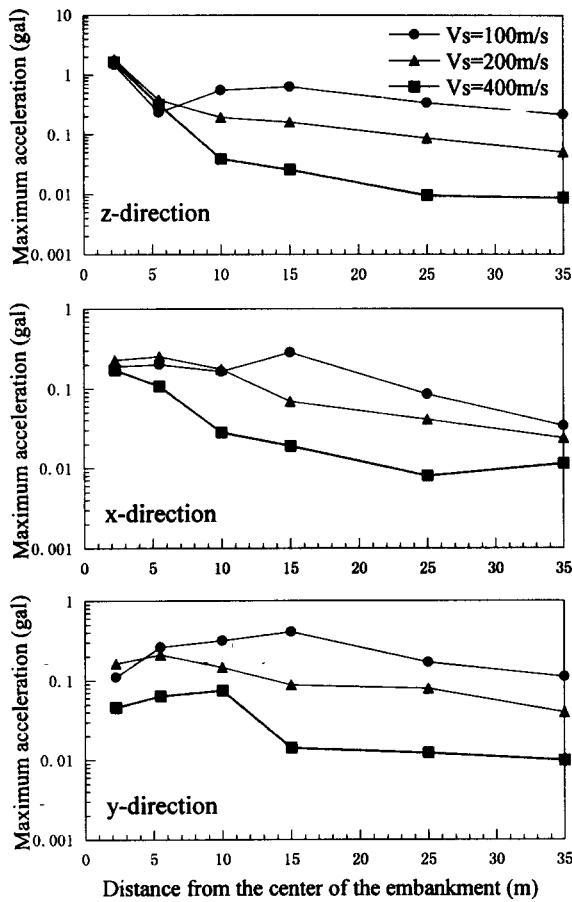
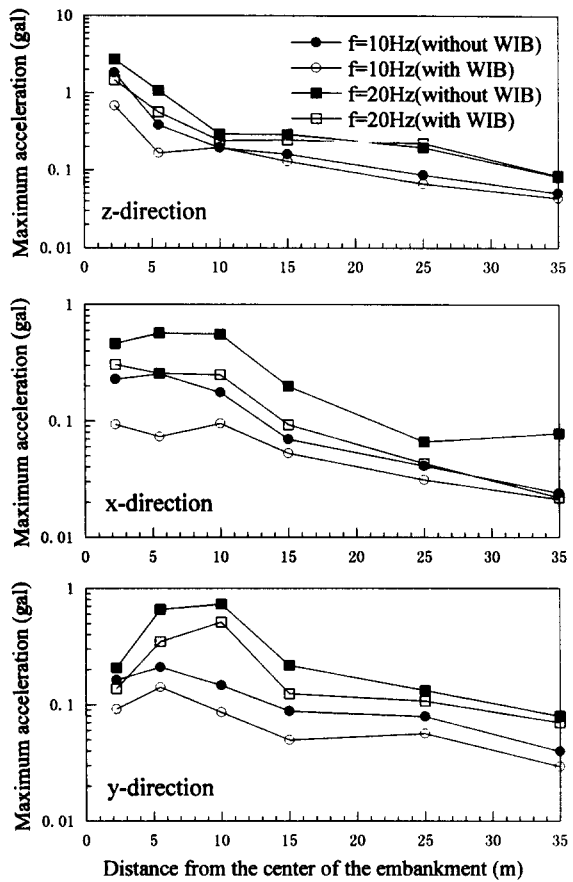Fig. 6 Maximum acceleration along the ground surface due to a unit patch load

Fig. 7 Maximum acceleration along the interface due to a unit patch load, Case 2(Vs=200m/s)

5. FIELD MEASUREMENT AND PREDICTION

The field measurement of the ground vibration was conducted for the Shinkansein operation. Fig.8 is the sketch for the track and the underlain soil conditions. Table 2 provides the Shinkansen train loads.

Table 2 Shinkanse train loads

Type	Weight per vehicle(kN)	Velocity (km/h)	Weight per axle (kN)
0	630	200～222	160
100	620	203～214	160
300	440	252～254	110

Fig.9 gives the recorded time histories and Fig.10 the corresponding Fourier amplitudes of the z-directional acceleration from the measurements for the 300-type 16
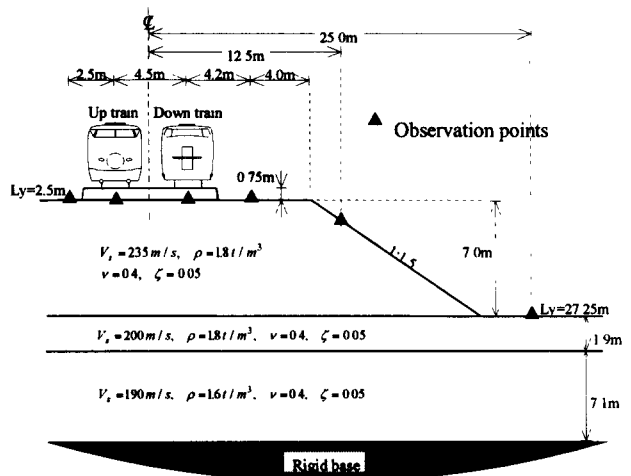

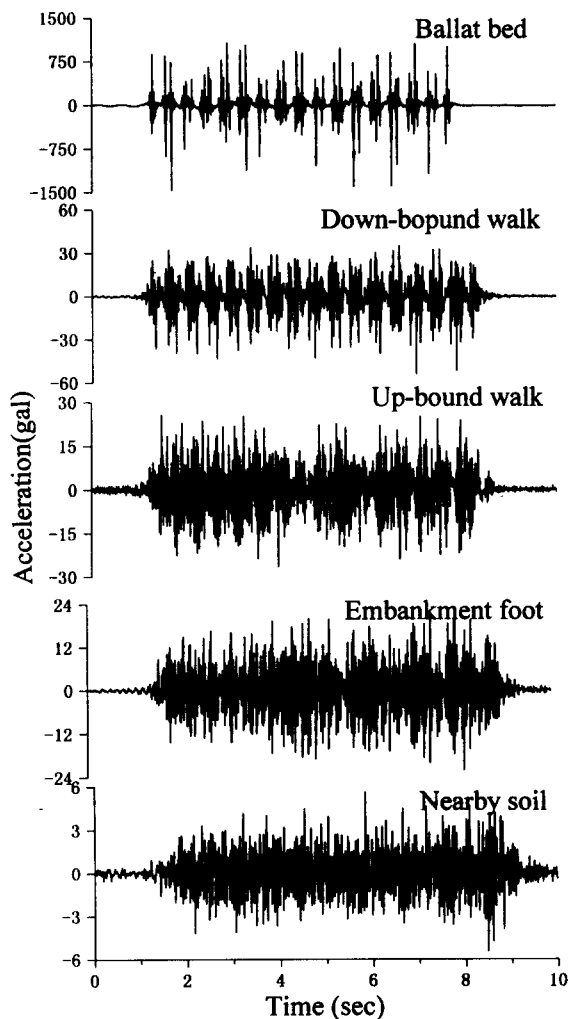Fig.8 Embankment typpe train track and underlain soils at measurement site

Fig.9 Time histories of acceleration measurements (z-component) for up-train 300 type (c=244 km/h)
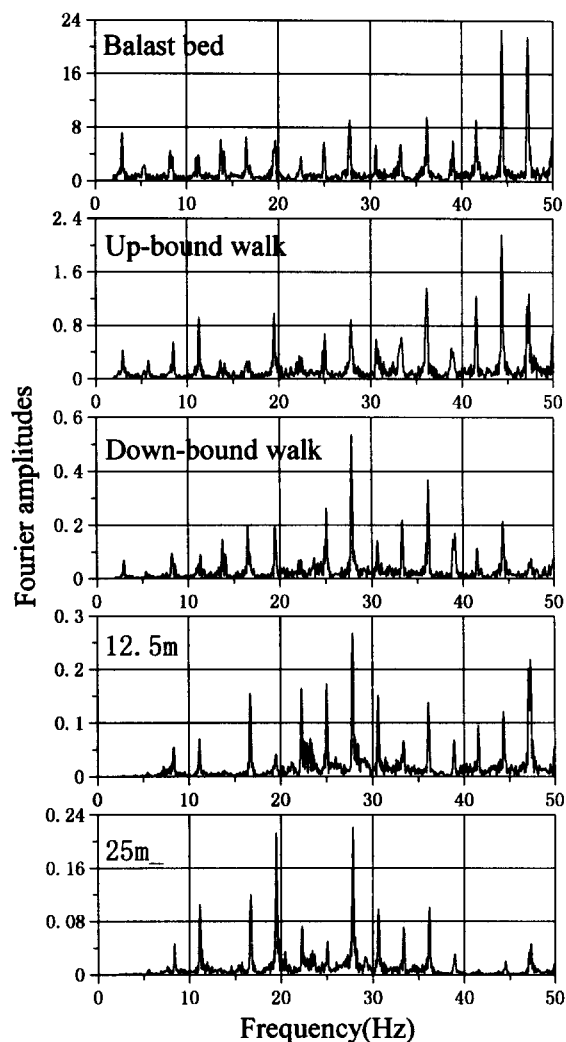

Fig. 10 Fourier amplitude of acceleration measurements (z-component) for up-train, 300 type (c=244 km/h)

cars train. The measurement data indicate different frequency contents depending on the location. On the track they indicate higher frequencies than 40 Hz, which is supposed to be caused by the unalignment of the rails appear while away from the track they show the predominant frequencies ranging 20 to 30 Hz results.

In order to improve the vibration prediction a specific weighting factor a_j is considered for the source loads so as to match the simulation with the measured data at selected frequencies.

$$f(x,y,t) = \Phi(x)\Psi(y)\sum_j a_j \exp(i\omega t) \qquad (8)$$

Fig.11 shows the observed maximum accelerations at distances from the track center for different types of Shinkansen and also depicts the simulation results through the above mentioned procedure in the range of 2.5m to 27.5m for the z-direction. The vibration intensity differs slightly by the type of Shinkansen. It is stated that taking an inverse analysis leads a reasonable prediction of vibrations induced by the train running.
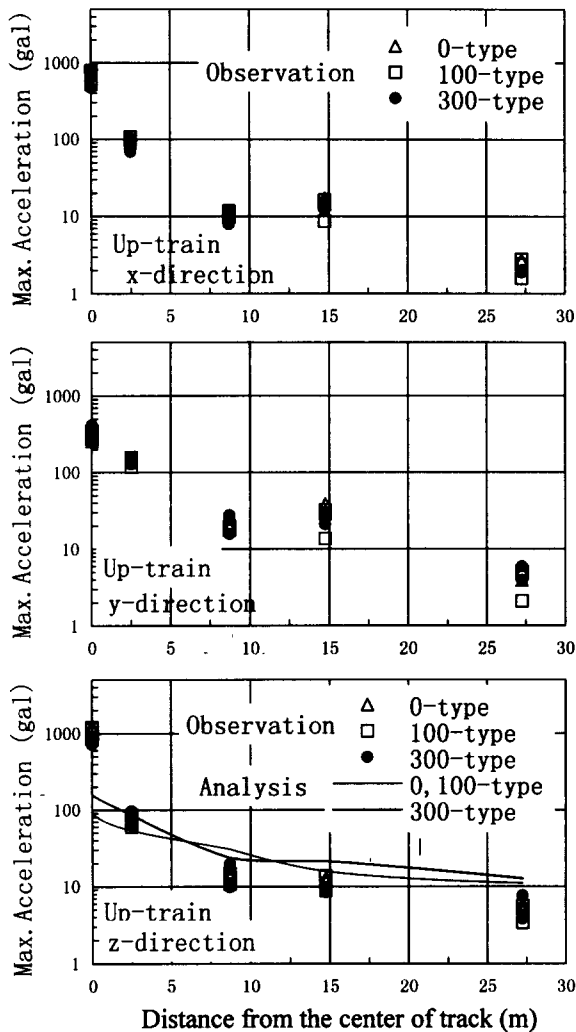
Fig.11 Attenuation of the maximum acceleration

6. CONCLUSION

Assessing the ground vibrations induced by the train running is of special importance from the environmental aspect.

Herein, the related computer simulation, based on the 2.5-dimensional FEM and BEM hybrid procedure, for the embankment train track were demonstrated. The fundamental parameter study for a moving patch load revealed the vibration characteristic of the embankment type train track and the vicinity, which differs depending on the relative stiffness between the embankment and the underlain soil layer. The vibration reduction is confirmed for a wave impeding block (WIB)installation inside the embankment.

Since the actual vibration from the train running includes various vibration sources, their contribution ratio was effectively determined by solving the inverse problem for the proposed model by claiming the response matching. The field measurement for the Shinkansen running was therefore conducted whose data are used for the for the better vibration prediction.

REFERENCES

1) Takemiya, H. and Goda, K.: 3-D transient response characteristics of soil stratum due to moving loads, Procs, Japan Society of Civil Engineers, No.563/I-39, 137-148, 1997.4 (in Japanese)

2) Takemiya, H. and Goda, K.: 3-D nonstationary response of a multilayered soil due to surface moving load, Procs, Japan Society of Civil Engineers, preparation for publication in JSCE (in Japanese)

3) Yoshioka, O.: Fixed source, moving source and generalized Doppler effects, Butsuri-Tansa, 48.2, 107-128, 1995 (in Japanese)

4) Yoshioka, O. Ashiya, K.: A dynamic model on excitation and propagation of Shinkansen-induced ground vibrations, Butsuri-Tansa, 48.5, 299-315, 1995 (in Japanese)

5) Takemiya, H., Goda, K and Komori, D.: Vibration chracteristics of embankment type track and its vicinity due to high-speed train running, Procs, Japan Society of Civil Engineers, preparation for publication in JSCE (in Japanese)

6) Takemiya,H., Shim, K-S, and Goda,K.: Embankment train track on soil stratum and wave impeding block (WIB) measured for vibration reduction , Procs of soil Dynamics and Earthquake Engineering VII , Computational Mechanics Pahlications, 1995,Creta 105-112